

## Research Article

# Performance Analysis of Natural $\gamma$ -Ray Coal Seam Thickness Sensor and Its Application in Automatic Adjustment of Shearer's Arms

Zengfu Yang <sup>1</sup>, Zengcai Wang <sup>2</sup>, and Ming Yan <sup>2</sup>

<sup>1</sup>CHN Energy Shandong Technology Research Institute, Shenmu 719300, China

<sup>2</sup>College of Mechanical Engineering, Shandong University, Jinan 250061, China

Correspondence should be addressed to Zengcai Wang; wangzc@sdu.edu.cn

Received 10 May 2020; Revised 6 July 2020; Accepted 5 August 2020; Published 25 August 2020

Academic Editor: Gurvinder S. Virk

Copyright © 2020 Zengfu Yang et al. This is an open access article distributed under the Creative Commons Attribution License, which permits unrestricted use, distribution, and reproduction in any medium, provided the original work is properly cited.

The technology of coal-rock interface recognition is the core of realizing the automatic heightening technology of shearer's rocker. Only by accurately and quickly identifying the interface of coal and rock can we realize the fully automatic control of shearer. As the only one used in the actual detection of coal mining machine drum cutting coal seam after the thickness of the remaining coal seam detection method, natural  $\gamma$ -ray has a very practical advantage. Based on the relationship between the attenuation of the natural  $\gamma$ -ray passing through the coal seam and the thickness of the coal seam, the mathematical model of the attenuation of the natural  $\gamma$ -ray penetrating coal seam is established. By comparing the attenuation intensity of  $\gamma$ -ray with or without brackets, it is verified that the hydraulic girders will absorb some natural  $\gamma$ -rays. Finally, this paper uses the ground simulation experiment and the field experiment to verify the correctness of the mathematical model and finally develop the natural  $\gamma$ -ray seam thickness sensor. The sensor has the function of indicating the thickness of the coal seam, measuring the natural  $\gamma$ -ray intensity, and storing and processing the data.

## 1. Introduction

Coal is the main energy source in China; the safe and efficient mining of coal is important for China's economic development. With the rapid development of modern control technology and the improvement of coal mining face automation, underground coal mining work has achieved high yield and high efficiency [1, 2]. But how to achieve the underground unmanned longwall face automation mining has always plagued the researchers. Coal mining machine as a key tool for coal mining face, how to achieve its automatic control is of great significance. To achieve fully automatic control of the shearer, we must first solve the problem of how to accurately determine the interface of coal and rock; only in this way, we can effectively solve the problem of shearer cutting drum increase automatically according to the coal seam ups and downs.

At present, it is judged that the interface between the coal and the rock is mainly controlled by the eye of the operator and the cutting sound to judge whether the cutting is a coal seam or a rock formation, so as to manually adjust the drum height. Then, due to the fact that the underground coal mining face environment is very bad, with large coal dust and low visibility, the eye observation to judge will lead to a large occurrence of a miscarriage of justice. The noisy environment of the scene also makes the cutting sound cannot be judged as an effective condition. The method of judging the interface between the coal and the workers is not only easy to reduce the use cycle of the cutting gear, increase the possibility of the gas explosion, decrease the quality of the coal and so on, but also greatly threaten the safety of the workers in the field. Therefore, it is of great significance to realize the precise identification of the interface of coal and rock, so as to realize the fully automatic control of unmanned face.

For decades, many countries' research institutions and researchers have made a lot of meaningful ways to accurately identify coal and rock interfaces. These methods are mainly divided into the detection method based on coal seam thickness and the detection method based on the coal-rock interface. The detection method based on coal seam thickness mainly includes an artificial  $\gamma$ -ray method [3, 4] and a natural  $\gamma$ -ray method [5, 6]. Based on the detection method of the coal-rock interface, there are radar detection method [7], passive infrared detection method [8], the cutting stress method [9, 10], the mechanical vibration method [11, 12], the image method [13–15], and other methods.

However, because the artificial  $\gamma$ -ray method will cause harm to the human body, it has been abandoned for a long time; the radar detection method does not apply to the thick coal seam face; the passive infrared detection method is more sensitive to ambient temperature. Cutting stress method's accuracy is not high enough; the mechanical vibration method is more susceptible to interference due to the underground transport machine vibration and other noisy sounds and due to underground dust and low visibility, making the camera shooting have poor results. In addition, there is often water or slime in the fieldwork, because of the mud cover, making coal and gangue more difficult to distinguish.

$\gamma$ -ray is a kind of electromagnetic radiation with short wavelength and high frequency. The wavelength is  $1.4 \times 10^{-9} \sim 5 \times 10^{-11}$  cm. The energy of  $\gamma$ -ray of natural radioactive elements is generally tens of keV to several MeV. Natural  $\gamma$ -ray can be radiated from both rock and coal seams, and the intensity of  $\gamma$ -ray radiation in rock stratum is much greater than that in the coal seam. Reference [16] identifies the gangue mixed in the top-coal caving when it is drawn by measuring the  $\gamma$ -ray radiation intensity in the process of top-coal caving. The natural  $\gamma$ -ray method can measure the residual radiation intensity of  $\gamma$ -ray from rock stratum after the attenuation of the coal seam, and the thickness of the top-coal seam can be determined according to its attenuation law, so as to achieve the purpose of coal-rock interface identification. And the natural  $\gamma$ -ray method is the only way to be applied to the actual mining industry so far. Although the natural  $\gamma$ -ray method was used in coal mines in the United Kingdom and the United States in the 1980s, there were differences in the radioactivity of coal and top-bottom rocks, the stability of coal ash, and the stability of top-bottom rocks in Chinese coal mines and Anglo-American mines. The natural  $\gamma$ -ray detector designed by British and American countries cannot be well applied to the Chinese coal mines; China in particular needs to design a natural  $\gamma$ -ray residual coal thickness detector which is in line with the situation of the Chinese coal mine.

In this paper, the mathematic model of the interface identification of coal and rock is proposed by establishing the relationship between the natural  $\gamma$ -ray attenuation intensity and the thickness of the coal seam, the presence of the brackets, and the natural  $\gamma$ -ray attenuation law. Using the ground simulation experiment and field experiment, the correctness of the data model is verified and finally developed into a natural  $\gamma$ -ray coal thickness sensor.

## 2. Materials and Methods

**2.1. Derivation of Attenuation Law of Natural  $\gamma$ -Ray through Coal Seam.** In the coal mining face, after the shearer worked, the coal seam can be left, and there is a roof rock natural  $\gamma$ -ray radiation through the coal seam. Natural  $\gamma$ -ray through the coal seam has a certain attenuation law; this section deduced the attenuation law, so as to provide a theoretical basis for sensor design and development. Figure 1 shows the radiation pattern of the radiation on the coal face. Assuming that the thickness of the ABCD at the top and bottom of the rock is  $l$ , the radioactive material (mainly uranium, thorium, and potassium) in the rock is uniform. There is a coal seam with a thickness of  $h$  below the rock. The instrument on the point  $P$  was measured. Since the attenuation of the  $\gamma$ -ray in the air is weak, the attenuation in the air below the coal seam is ignored. The concentration of radioactive material in the rock is expressed by  $q$  Curie/g, the attenuation coefficient of the radioactive material  $\gamma$ -ray in the rock itself is expressed by  $k$ , and the attenuation coefficient in the coal seam is expressed by  $\mu$ . The thickness of the hydraulic support roof beam is  $h_0$ . The attenuation coefficient of the beam of the hydraulic support roof beam is  $\mu_e$ .

In the rock, we take an infinitesimal volume  $dv$  (parallelepiped  $b-c-d-e-i-l-m-n$ ), the volume of radiation emitted through the rock thickness is  $bf = r - r_2$ , through the thickness of the coal seam, it is  $fg = r_2 - r_1 = h \sec \Psi$ , and through the hydraulic support column, the steel plate thickness is  $g_0g = h_0 \sec \Psi_0$ .

When the ray passes through the rock and the coal seam, the radiation intensity of the voxel  $dv$  at the point  $p$  is shown in the following expression:

$$dJ = K' \frac{q\rho dv}{r^2} e^{-k(r-r_2)} \cdot e^{-\mu(r_2-r_1)}, \quad (1)$$

where  $K'$  is the proportionality coefficient and  $\rho$  is the rock density.

When the ray passes through the rock, coal crust, and support beam steel plate, the radiation intensity produced by the voxel  $dv$  at the point  $p$  is shown in the following expression:

$$dJ = K' \frac{q\rho dv}{r^2} e^{-k(r-r_2)} \cdot e^{-\mu(r_2-r_1)} e^{-\mu_e(r_1-r_4)}. \quad (2)$$

As can be seen from Figure 1,

$$dv = r^2 \sin \psi d\psi dr. \quad (3)$$

Due to the attenuation of natural gamma rays by hydraulic support beam steel plate, for the case of Figure 1, the expression (4) of radiation intensity  $J_h$  of point  $p$  is as follows:

$$J_h = (J - J_p) + J_e. \quad (4)$$

The physical meaning of this formula is that after the natural  $\gamma$ -ray passes through the coal seam and the top beam of the brackets, the radiation intensity  $J_h$  at point  $p$  is

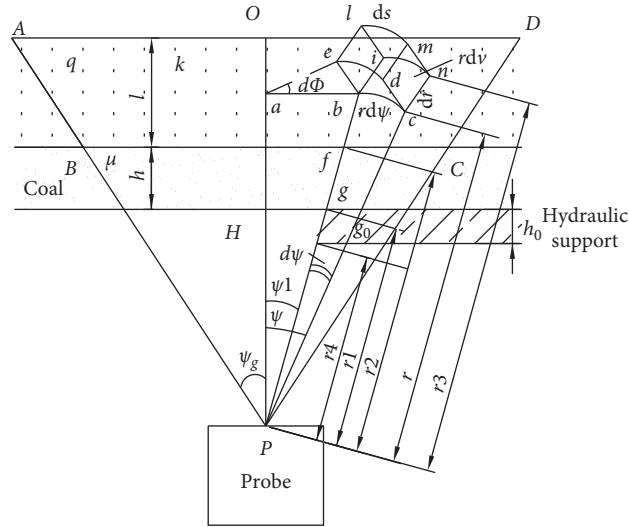


FIGURE 1: Radiation of natural  $\gamma$ -ray passing through coal seam and hydraulic support roof beam.

decomposed into two parts, part of which is the radiation intensity  $J - J_p$  of the coal passing through the uncoated roof beam and the other part is the radiation intensity  $J_e$  of the beam and the top beam of the brackets covered by the brackets, where we have the following.

$J$  is the radiation intensity of the natural  $\gamma$ -ray passing through the coal seam at the point  $p$  in the absence of hydraulic support, as described in [17]

$$J = \frac{2\pi K' q\rho}{k} \Phi(\mu h) - \cos \psi_0 \Phi(\mu h \sec \psi_0) - \Phi(\mu h + kl) + \cos \phi_0 \Phi[(\mu h + kl) \sec \phi_0]. \quad (5)$$

$J_p$  is the radiation intensity of the natural  $\gamma$ -ray which is in the rock at the top of the hydraulic support roof beam through the coal seam at the point  $p$ .

$J_e$  is the radiation intensity of the natural  $\gamma$ -ray which is in the rock at the top of the hydraulic support roof beam through the coal seam and bracket top beam at the point  $p$ .

$J - J_p$  is the intensity of the radiation at the point  $p$  after the natural  $\gamma$ -ray through the coal seam in the part of the rock that is not covered by the hydraulic support.

Next, the expression of  $J_p$  and  $J_e$  can be derived from Figure 1, where the expression is as follows:

$$J_p = K' q\rho \int_{-\theta_0}^{\theta_0} d\varphi \int_{\psi_1}^{\psi_0} e^{-\mu h \sec \psi} \sin \psi d\psi \int_{r_2}^{r_3} e^{-k(r-r_2)} dr. \quad (6)$$

Substituting  $r_2 - r_3 = l \sec \Psi$  into (6) and introducing the Ginger function [18] yield the expression (7) as follows:

$$J_p = \frac{2\theta_0 K' q\rho}{k} \{\cos \psi_1 \Phi(\mu h \sec \psi_1) - \cos \psi_0 \Phi(\mu h \sec \psi_0)\} - \frac{2\theta_0 K' q\rho}{k} \{\cos \psi_1 \Phi[(\mu h + kl) \sec \psi_1] - \cos \psi_0 \Phi[(\mu h + kl) \sec \psi_0]\}. \quad (7)$$

The expression of  $J_e$  is shown by the following equation:

$$J_e = K' q\rho \int_{-\theta_0}^{\theta_0} d\varphi \int_{\psi_1}^{\psi_0} e^{-\mu h \sec \psi} e^{-\mu_e h_0 \sec \psi} \sin \psi d\psi \int_{r_2}^{r_3} e^{-k(r-r_2)} dr. \quad (8)$$

Similarly, substituting  $r_2 - r_3 = l \sec \Psi$  into (8) and introducing the Ginger function yield the expression (9) as follows:

$$J_e = \frac{2\theta_0 K' q\rho}{k} \{\cos \psi_1 \Phi[(\mu h + \mu_e h_0) \sec \psi_1] - \cos \psi_0 \Phi \cdot [(\mu h + \mu_e h_0) \sec \psi_0]\} - \frac{2\theta_0 K' q\rho}{k} \{\cos \psi_1 \Phi[(\mu h + \mu_e h_0 + kl) \sec \psi_1] - \cos \psi_0 \Phi \cdot [(\mu h + \mu_e h_0 + kl) \sec \psi_0]\}, \quad (9)$$

where  $\theta_0$  is the angle occupied by the projection of the cover of the hydraulic support in the plane and  $\psi_1$  is the angle between the centerline of the radiation cone and the edge of the top beam of the hydraulic support.

The above results deduce the radiation intensity formula of the natural  $\gamma$ -ray in the upper rock of the top of the hydraulic support through the coal seam and through the coal seam and the support beam. The derivation analysis of these key parameters can get the attenuation law of the ray.

## 2.2. Effect of Brackets on the Attenuation of Natural $\gamma$ -Rays.

In the previous section, the formulas of natural  $\gamma$ -ray radiation intensity in the case of no roof beam and with roof beam are derived, respectively. After determining other parameters, the variation law of  $\gamma$ -ray radiation intensity with coal seam thickness can be obtained. Because the comprehensive mining face is covered by hydraulic support, the radiation intensity of natural  $\gamma$ -ray, which passes

through the roof rock of the hydraulic support beam, is affected. Therefore, for the more complicated ray attenuation in coal mining face, through the numerical calculation of formulas (4) to (9), the attenuation law of natural  $\gamma$ -ray can be obtained under two different conditions, namely, the bracket beam and the nonsupport beam roof. By comparing the difference between them, the influence of the support roof beam on the measurement accuracy of the coal seam thickness is analyzed.

In the study of the effect of brackets on the attenuation of natural  $\gamma$ -rays, respectively, we take  $\mu = 0.0075$ ,  $k = 0.0167$ ,  $l = 600$  mm,  $\mu_e = 0.0585$ ,  $h_0 = 41$  mm, and  $\rho = 2.63$  g/cm<sup>3</sup>, and we take  $\psi_0 = 60^\circ$  and  $\psi_0 = 45^\circ$ , corresponding to  $\psi_1 = 50^\circ$  and  $\psi_1 = 35^\circ$ . After setting these parameters, we carry out the calculation and analysis, and we will get the radiation intensity  $J$  and  $J_h$  with the variation of  $h$  in the law shown in Figure 2. Among them, curve 1 is the attenuation law when the support roof beam exists, and  $\psi_0 = 45^\circ$  and  $\psi_1 = 35^\circ$ . Curve 2 is the attenuation law when the support roof beam does not exist, and  $\psi_0 = 45^\circ$  and  $\psi_1 = 35^\circ$ . Curve 3 is the attenuation law when the support roof beam exists, and  $\psi_0 = 60^\circ$  and  $\psi_1 = 50^\circ$ , and curve 4 is the attenuation law when the support roof beam does not exist, and  $\psi_0 = 60^\circ$  and  $\psi_1 = 50^\circ$ .

It can be seen from the curve in Figure 2 that the natural  $\gamma$ -ray radiation intensity gradually decreases with the increase of coal seam thickness, but the variation gradient of the curve decreases with the coal seam thickness. Therefore, the natural gamma-ray method can be used to detect the thickness of the remaining coal seam, but in order to have sufficient detection resolution, the thickness of the coal seam which can be detected by the natural  $\gamma$ -ray method is a certain range.

By comparing curve 1 and curve 2 and curve 3 and curve 4, it can be seen that the radiation intensity of the natural  $\gamma$ -ray is basically the same in the case of no support roof beam and with the brackets, but there is a certain error between them. The occurrence of this error is that the brackets have a certain attenuation effect on the radiation, and the  $\gamma$ -ray radiation intensity will be reduced in the case of hydraulic support top beam. In order to improve the measurement accuracy of coal seam thickness, the influence of the steel beam on the attenuation of the beam should be considered. In particular, when the brackets are thicker, the influence of the brackets on the radiation attenuation should be considered.

### 2.3. Error and Accuracy Analysis of Natural $\gamma$ -Ray Measurement

**2.3.1. Statistical Distribution of Natural  $\gamma$ -Ray Measurements.** Since the decay of the nucleus is completely random, it is governed by the probability law [19]. Therefore, even when the source intensity, the attenuation medium, the measuring instrument, and the measurement conditions are constant during the natural  $\gamma$ -ray measurement, the result  $N$  of each measurement is not the same at the same time interval, but around an average value of  $B$  fluctuation, this

phenomenon is called radioactive fluctuation or radioactive ups and downs. The error between the result of each measurement and the mean of the natural  $\gamma$ -ray is denoted as  $\Delta N = N - \bar{N}$ . To investigate the statistical distribution of ray measurements, we assume that the number of natural  $\gamma$ -ray radionuclides is  $N_0$ , and the distribution of the probability of the number of  $N$  nuclei decay is deduced after  $t$  time, and it can be expressed by  $W(N)$ .

If the probability of a kernel in a certain period of time is  $p$ , then the probability of no decay that occurs within this time is  $q = 1 - p$  and  $p + q = 1$ .

During this time, from the number of  $N_0$  nuclear decay out of the number of  $N$  nuclei, there is a possibility that a total of  $C_{N_0}^N$  from the  $N_0$  takes the arrangement of  $N$  expressed as

$$C_{N_0}^N = \frac{N_0!}{(N_0 - N)!N!} \quad (10)$$

Because the possibility that the number of  $N$  radionuclides decays at the same time is  $p^N$  and the possibility that the number of  $N_0 - N$  nuclides does not decay is  $q^{(N_0 - N)}$ , so in each kind of  $C_{N_0}^N$  combination, in each kind of request, the possibility that the number of  $N$  nuclei decays and  $N_0 - N$  nuclei at the same time does not decay is as shown in the following expression:

$$W(N) = C_{N_0}^N p^N q^{N_0 - N}. \quad (11)$$

The average number of decay is

$$\bar{N} = pN_0. \quad (12)$$

Substituting expression (12) into expression (11), we can get the expression (13) as follows:

$$\begin{aligned} W(N) &= \frac{1 \cdot 2 \cdot 3 \cdots (N_0 - 1)N_0}{N! \cdot 1 \cdot 2 \cdot 3 \cdots (N_0 - 1)} \left(\frac{\bar{N}}{N_0}\right)^N \cdot \left(\frac{N_0 - \bar{N}}{N_0}\right)^{N_0 - N} \\ &= \frac{(N_0 - N + 1) \cdots (N_0 - 1)N_0}{N!} \left(\frac{\bar{N}}{N_0}\right)^N \left(\frac{N_0 - \bar{N}}{N_0}\right)^{N_0 - N} \\ &= \left(1 - \frac{N - 1}{N_0}\right) \left(1 - \frac{N - 2}{N_0}\right) \cdots \left(1 - \frac{1}{N_0}\right) \frac{\bar{N}^N}{N!} \\ &\quad \cdot \left(\frac{N_0 - \bar{N}}{N_0}\right)^{N_0 - N}. \end{aligned} \quad (13)$$

Assuming that  $N_0$  is very large, then the limit value of  $N_0 \rightarrow \infty$  is expressed as

$$W(N) = \frac{\bar{N}^N}{N!} \lim_{N_0 \rightarrow \infty} \left(1 - \frac{\bar{N}}{N_0}\right)^{N_0 - N} = \frac{\bar{N}^N}{N!} e^{-\bar{N}}. \quad (14)$$

As can be seen from equation (14), the distribution of natural  $\gamma$ -ray at this time is consistent with the Poisson distribution. The natural  $\gamma$ -ray thickness sensor will be designed according to the distribution of the ray.

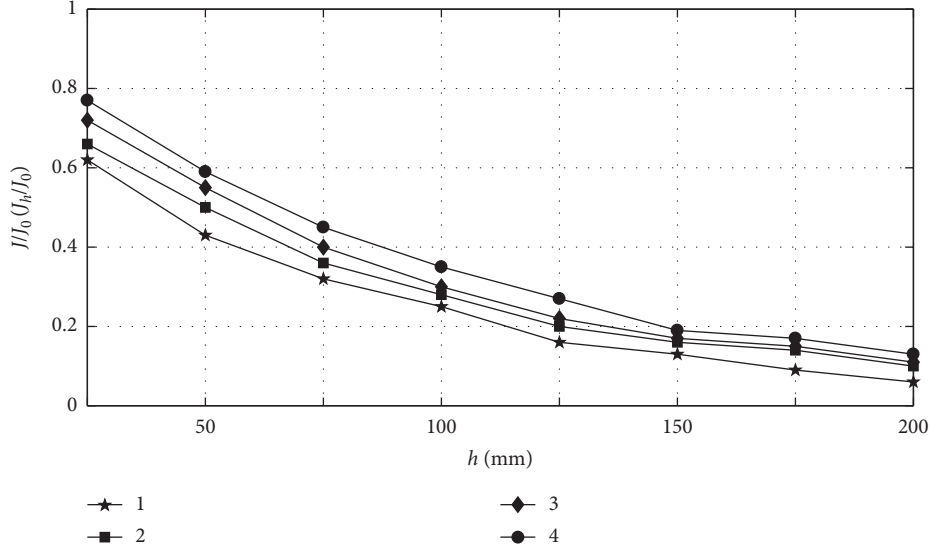


FIGURE 2: Variation curve of  $\gamma$ -ray radiation intensity with coal seam thickness in case of considering the influence of the top beam and without considering the influence of the top beam.

2.3.2. *Distribution Rule of Natural  $\gamma$ -Ray Measurement Errors.* The study of natural  $\gamma$ -ray measurement error is very important for the improvement of the measurement accuracy of the sensor. Through the research of the distribution law, the key factors that can affect the measurement accuracy can be obtained, and then the precision of the measurement sensor can be improved by controlling the key parameters. According to the probability theory [20], we can find the deviation between the measured value and the mean value, so as to find out the distribution rule of the natural gamma-ray measurement observation error.

In statistics, the deviation  $\Delta N$  between the observed  $N$  and the mean  $\bar{N}$  can be positive and negative, and the positive and negative deviations formed in the infinite number of observations are equal; that is, the mean deviation is zero, which loses the meaning of the error representation. The average deviation cannot be used to represent the accuracy of the observations; by definition, the mean square error is expressed as

$$\sigma = \sqrt{\overline{(\bar{N} - N)^2}} = \sqrt{\frac{\sum_{i=1}^m (\bar{N} - N_i)^2}{m}}, \quad (15)$$

where  $A$  is the  $i$  th observed value and  $m$  is the number of observations.

The square of the mean square error is the mean square deviation, which is called the variance, and its expression is as follows:

$$\sigma^2 = \overline{(\bar{N} - N)^2} = \frac{1}{m} \sum_{i=1}^m (\bar{N} - N_i)^2. \quad (16)$$

Next, the values for calculating the variance and the mean square error can be expressed by the following expression.

According to the average definition, we get the following expression:

$$\bar{N} = \sum_{N=1}^{N_0} NW(N). \quad (17)$$

The following expression (18) is given by expressions (11) and (12):

$$W(N) = \frac{N!}{(N_0 - N)!N!} p^N q^{N_0 - N}. \quad (18)$$

Expanding  $\sigma^2 = \overline{(N - \bar{N})^2}$ , we can get the following expression:

$$\sigma^2 = \overline{N^2 - 2N\bar{N} + (\bar{N}^2)} = \bar{N}^2 - (\bar{N})^2. \quad (19)$$

In expression (19),

$$\bar{N}^2 = \sum_{N=1}^{N_0} N^2 W(N). \quad (20)$$

Next, we calculate the value of  $\sigma^2$ , due to

$$W(N) = \frac{N_0!}{(N_0 - N)!N!} p^N q^{N_0 - N} C_{u^N} (pu + q)^{N_0}, \quad (21)$$

where  $C_{u^N} (pu + q)^{N_0}$  is the coefficient of  $u^N$  in the expansion  $(pu + q)^{N_0}$ ; therefore, the expression (22) can be got as follows:

$$\begin{aligned} \bar{N} &= \sum_{N=1}^{N_0} N \cdot C_{u^N} (pu + q)^{N_0} \\ &= \sum_{N=1}^{N_0} \left[ \frac{d}{du} C_{u^{N-1}} (pu + q)^{N_0} \right] \\ &= \left[ \frac{d}{du} (pu + q)^{N_0} \right]_{u=1} \\ &= N_0 p (p + q)^{N_0 - 1} \\ &= N_0 p. \end{aligned} \quad (22)$$

Similarly,

$$\begin{aligned}\bar{N}^2 &= \sum_{N=1}^{N_0} N^2 \cdot C_{u^N} (pu + q)^{N_0} \\ &= \sum_{N=1}^{N_0} \left\{ \frac{d}{du} \left[ u \frac{d}{du} C_{u^{N-1}} (pu + q)^{N_0} \right] \right\} \\ &= \left\{ \frac{d}{du} \left[ u \frac{d}{du} C_{u^{N-1}} (pu + q)^{N_0} \right]_{u=1} \right\} \\ &= N_0 p + N_0 (N_0 - 1) p^2.\end{aligned}\quad (23)$$

Substituting expression (22) into (19) yields the expression (24) as follows:

$$\sigma^2 = N_0 p + N_0 (N_0 - 1) p^2 - (N_0 p)^2 = N_0 p (1 - p) = N_0 p q. \quad (24)$$

Substituting  $p = \bar{N}/N_0$  and  $q = 1 - p = 1 - (\bar{N}/N_0)$  into (24) yields the expression (25) as follows:

$$\sigma^2 = \bar{N} \left( 1 - \frac{\bar{N}}{N_0} \right). \quad (25)$$

We assume  $N_0 \gg \bar{N}$ , so we can know  $\sigma^2 = \bar{N}$ , and the expression (26) is also established:

$$\sigma = \sqrt{\bar{N}} \approx \pm \sqrt{N}. \quad (26)$$

The mean square error is an absolute error. The influence of the observation accuracy is expressed by the relative error in the statistical law. By definition, the relative error which is also called the mean square error is expressed as follows:

$$\delta = \pm \frac{\sigma}{\bar{N}} \approx \pm \frac{1}{\sqrt{N}}. \quad (27)$$

From expression (27), we can see that the relative mean square error of natural  $\gamma$ -ray counting is

$$\delta = \pm \frac{1}{\sqrt{N}}. \quad (28)$$

According to the formula of measurement error of natural  $\gamma$ -ray, it is known that in order to improve the measurement accuracy, improve the counting, and ensure the sufficient count and the measurement result to achieve certain accuracy, five methods can be adopted. These five methods are to improve the sensitivity of the sensor, to extend the measurement time, to increase the number of measurements, to reduce the measurement of the background count, and to increase the intensity of the radioactive source. These five methods can improve the count value to a certain extent, so as to achieve the purpose of improving the accuracy of natural  $\gamma$ -ray radioactivity measurement.

**2.4. Structural Design of the Measurement Sensor.** The natural  $\gamma$ -ray method is to determine the thickness of the coal by detecting the amount of  $\gamma$ -ray radiation emitted by some of the natural radioactive materials in the roof rock of the coal

seam. Because the coal seam has a certain density, it absorbs a certain amount of  $\gamma$ -rays, so the amount of  $\gamma$ -rays passing through the coal seam is directly related to the thickness of the coal seam. That is, the thicker the coal seam is, the less it passes through its  $\gamma$ -ray; the thinner the coal seam is, the more it passes through its  $\gamma$ -ray. In order to verify the accuracy of the mathematical model, this section focuses on the natural  $\gamma$ -ray coal thickness sensor developed on the basis of the abovementioned study and summarizes the relevant studies [21–23] for measuring the thickness of the remaining coal seam after shearing the coal seam, and meanwhile, its working principle, hardware circuit structure, and software program are introduced in detail.

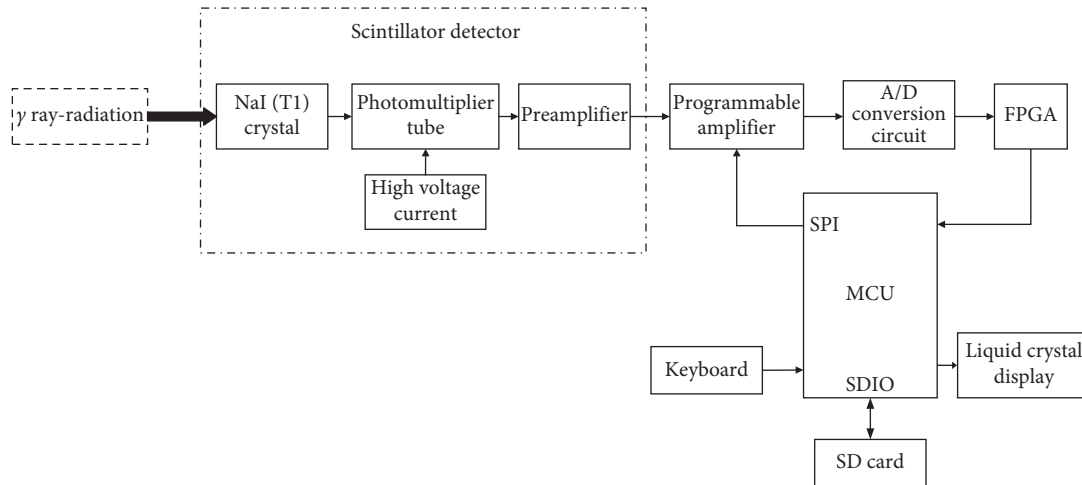
The structure of the natural  $\gamma$ -ray coal thickness sensor is shown in Figure 3. The sensor is mainly composed of a scintillator detector, program control amplifier, A/D conversion circuit, FPGA signal processing circuit, and microcontroller unit (MCU). FPGA is to complete natural  $\gamma$ -ray pulse counting, and MCU is to convert pulse count into coal skin thickness.

The scintillator detector is composed of NaI(Tl) crystal, photomultiplier tube, and preamplifier. When the  $\gamma$ -ray emitted by the radiation source enters the NaI(Tl) crystal in the detector, it will excite the crystal to emit light. The photons generated will knock out photoelectrons at the photocathode of the photomultiplier tube, and each photoelectron will knock out several electrons at the multiplier pole of the photomultiplier tube. These electrons will be converted into voltage pulse output after multiple times of multiplication. Usually, NaI(Tl) crystal and photomultiplier tubes are packed in a dark box. According to the conclusion in Section 3.2, in order to improve the measurement accuracy, it is necessary to extend the measurement time. Therefore, in order to improve the detection efficiency and sensitivity on the basis of ensuring the measurement accuracy, a larger crystal must be used. Taking into account funding constraints, the NaI (Tl) crystal size is  $\Phi 75 \times 75$  mm.

The pulse signal from the scintillator detector is weak and needs further amplification. The program controller is used as the main amplifier of the sensor; MCU can control the amplification factor of the program amplifier through SPI bus; the analog voltage signal of the electric pulse is converted into a digital signal by A/D conversion circuit; the digital signal is processed by FPGA analysis circuit such as filtering, shaping, stacking judgment, pulse amplitude extraction, energy spectrum information storage, and transmission. FPGA analysis circuit can realize the multichannel counting of pulse electric signal, and it is convenient to set the initial energy threshold. Only the appropriate initial energy threshold can meet the detection sensitivity requirements and anti-interference performance of the sensor. The experimental results show that the initial energy threshold of the sensor should be set at 30–70 keV.

### 3. Experiment and Analysis of Results

**3.1. Experimental Study on Natural  $\gamma$ -Ray Decay Curve of Coal Seam.** In order to verify the natural  $\gamma$ -ray attenuation curve

FIGURE 3: Natural  $\gamma$ -ray coal thickness sensor structure.

of the coal seam in the actual process, a simulation experiment site was made in the laboratory. The test site is set up as follows. The roof is replaced by granite with a length of 1000 mm, a width of 1000 mm, and a thickness of 600 mm. The granite is of medium radioactivity and its radioactivity is comparable to that of the top and bottom slag sandstone, limestone, mudstone, and sandstone in the coal mine. Radioactive content is up to  $5 \times 10^{-12} \sim 30 \times 10^{-12}$  grams of radium equivalent/g. A square with an area of  $750 \times 750$  mm is made of coal, the thickness of the coal seam is gradually changed by 21.8 mm, 39 mm, 72.2 mm, 113 mm, 166 mm, and 190 mm, and the initial threshold of the FD3003 spectrometer is changed. The initial thresholds are 60 keV, 100 keV, 200 keV, 300 keV, 400 keV, 500 keV, 600 keV, and 700 keV, respectively. The measured curves of the radiation intensity with the thickness of the coal seam at different initial thresholds are shown in Figure 4.

It can be seen from Figure 4 that the natural  $\gamma$ -ray passes through the coal seam and its radiation intensity gradually decays, but as the thickness of the coal seam increases, the natural  $\gamma$ -ray attenuation gradient becomes smaller. The experimental results show that the use of a natural  $\gamma$ -ray method for coal seam thickness measurement is feasible.

It can be seen from Figure 4 that when the coal seam is thick, the measured attenuation curve suddenly bent down; this part is not natural  $\gamma$ -ray inherent attenuation law, and the main reason for this trend is that the ray intensity is too weak, beyond the normally accepted sensitivity range of the instrument, resulting in a large reception error. Therefore, the maximum thickness of the coal seam measured by the natural  $\gamma$ -ray method is limited by the radioactive material contained in the rock and the sensitivity of the instrument.

**3.2. Algorithm Design of Natural Gamma Ray Coal Thickness Sensor Experiment.** According to the structural design of the natural  $\gamma$ -ray coal thickness sensor and the application in practical engineering, the design of the sensor is designed to meet the requirements of the actual measurement. The algorithm design is divided into three parts:

- (1) Timing control module: the main function of this part is to set the time for each measurement. Within the instrument, the minimum time interval controlled by the software is 1 s, and the time interval is entered by the timing control section. Each measurement time can be controlled to seconds
- (2) Measurement module: the module is the core module of the system. It collects the pulse count, calculates the corresponding coal thickness under the pulse count according to the decay curve, and displays the thickness value, the pulse count, and the corresponding coal seam thickness stored
- (3) Calibration module: calibration module is the role of the current situation for the  $\gamma$ -ray attenuation characteristics to find the attenuation characteristics of the regression curve. In the measurement process, the pulse count was measured through the regression curve to get the thickness of the coal seam. The module to complete the task is mainly the three representative points of the pulse count and the corresponding thickness of the coal into the memory unit.

The block diagram of the measurement module is shown in Figure 5. The main idea of the program is to calculate the thickness of the coal based on the pulse count. The decay curve in the program adopts the quadratic polynomial curve [19]. The equation expression is as shown in

$$y_i = ah_i^2 - bh_i + c, \quad (i = 1, 2, 3), \quad (29)$$

where  $y_i$  is the pulse count value and the  $h_i$  is the thickness of the coal seam.

Three linear equations can be obtained by calibrating the coefficient  $(y_i, h_i)$  for three times, and the coefficient  $a, b, c$  is obtained by solving the equation; also, the decay equation is obtained. In turn, formula (30) is obtained by the measured pulse count  $y_i$ :

$$h = \frac{b - \sqrt{b^2 - 4a(c - y)}}{2a}. \quad (30)$$

When the thickness data measured in the above equation is normal, the value can be stored in the corresponding

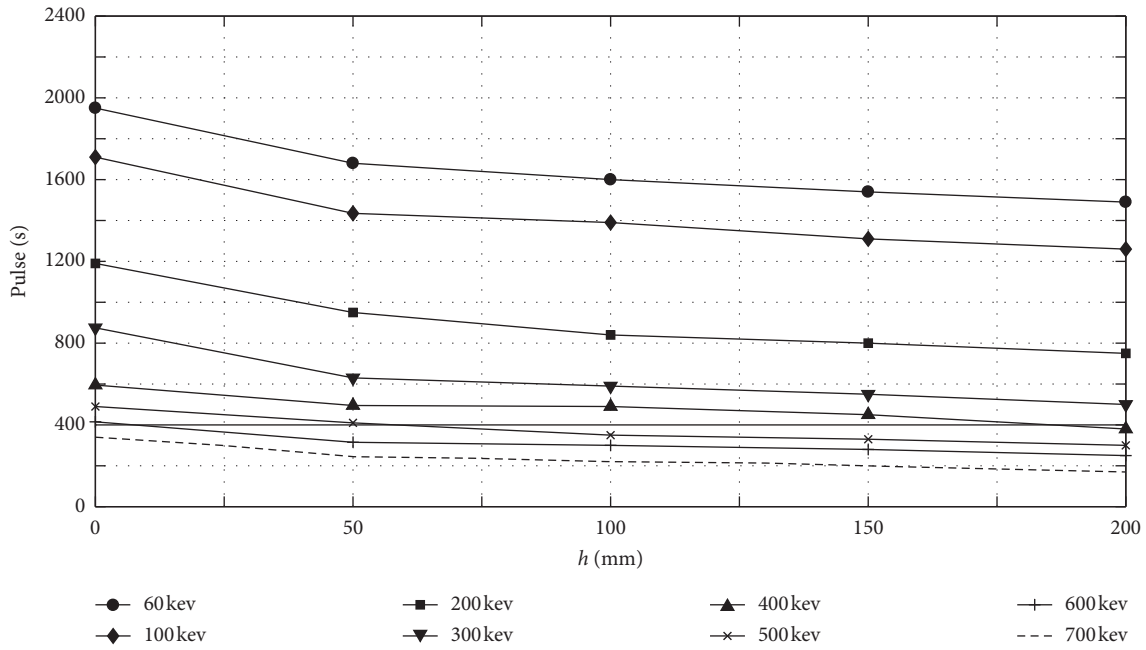


FIGURE 4: The measured natural  $\gamma$ -ray decay curves at different initial thresholds.

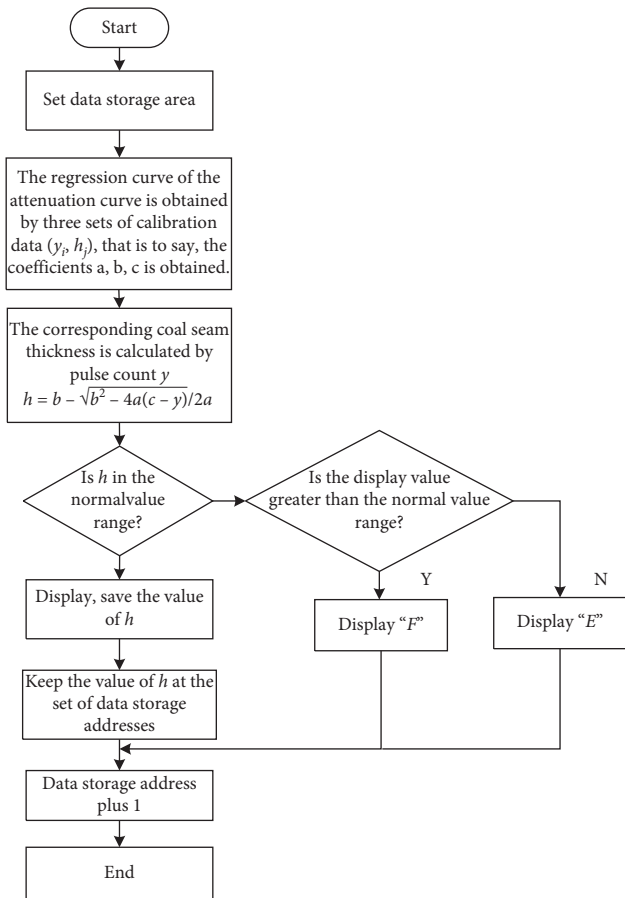


FIGURE 5: Block diagram of the measurement module.

memory cell by pressing the memory key on the keyboard. Also in the program, we set the thickness value to be in the normal range of the judge program; if the thickness value is

beyond the normal range, the display gives instructions to remind us to check the reasons for the inspection.

The calibration procedure is carried out using the corresponding calibration point. Three typical points are taken as calibration points in the measurement site. The program first measures the pulse count value corresponding to a calibration point, then the operator enters the coal thickness of the point into the program, and the program stores the pulse count at that point and its corresponding thickness of the coal into the storage unit. These three sets of data determine the three linear equations. The block diagram of the calibration module is shown in Figure 6.

This algorithm is designed to meet the three major functional requirements of timing control, measurement, and calibration, to realize whether the test data is normal, and to realize the storage function of the data, which can meet the requirement of data storage processing in the process of using the sensor.

*3.3. Measurement of Natural  $\gamma$ -Ray Coal Thickness Sensor in the Experiment.* The structure design and design of the natural  $\gamma$ -ray coal thickness sensor are introduced in detail. On this basis, the developed sensor is applied to the actual measurement to verify its feasibility and performance. In the experiment, the natural  $\gamma$ -ray coal thickness sensor is used to measure the thickness of the ground coal seam in the actual environment. The measurement results are shown in Table 1.

From Table 1, we can get the results: in the coal thickness range of 0–200 mm, the measured maximum absolute error is –18.9 mm. The maximum relative error is 13.5%. As the measurement of the thickness of the precision requirements is not high, generally within 20% of the relative error can meet the engineering requirements. So, this detection

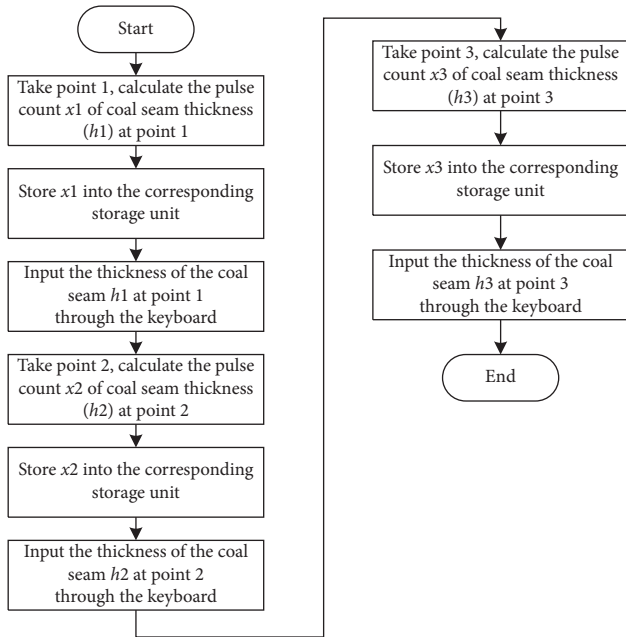


FIGURE 6: Block diagram of the calibration procedure.

TABLE 1: Analysis of coal seam thickness measurement error.

Count value (pulse/0.5 s)	222	193	186	167	157
Actual coal seam thickness (mm)	0	50	100	150	200
Instrument measurements value (mm)	-16.4	59	81.1	158	227
Absolute error value (mm)	-16.4	9	-18.9	8	27
Relative error value (%)	—	4.5	-9.5	4	13.5

accuracy can fully meet the coal mine to measure the thickness of coal to meet the requirements.

#### 4. Conclusion

This paper mainly introduces a natural  $\gamma$ -ray coal thickness sensor, which mainly applies the natural  $\gamma$ -ray to the actual thickness of the coal seam after cutting the coal seam. Through the simulation experiment and actual field experiment, finally, we verified the feasibility of the various functions of the sensor.

It is consistent with the natural  $\gamma$ -ray attenuation curve obtained by the calculation. That is, when the natural  $\gamma$ -ray passes through the coal seam, the radiation intensity gradually decays, but as the thickness of the coal seam increases, the gradient of the natural  $\gamma$ -ray decreases gradually. However, because of the experimental conditions, the radioactive material content of the experimental radioactive source (granite) is weak, so the experimental decay curve is weaker than the theoretical calculation of the attenuation curve. When the experimental curve is measured with a radioactive material with high radioactive content, the experimental curve will become steep. This will have a closer trend with the theoretical calculation of the attenuation curve. At the same time, it also shows that the theoretical derivation formula has great guiding significance.

The natural  $\gamma$ -ray is basically the same as in the case of no-beam and the top of the brackets, but the two cases have some differences. This error is generated by the attenuation of the beam on the brackets. Considering the attenuation of the natural beam by the top of the hydraulic support can get more accurate attenuation law, so as to improve the accuracy of coal thickness measurement.

On the basis of the theoretical research, the design of the natural  $\gamma$ -ray coal thickness sensor is tested and the maximum relative error is 13.5%, which can meet the engineering requirements of less than 20% of the relative error. The detection accuracy can meet the precision requirements in practical application.

#### Data Availability

The data used to support the findings of this study are available from the corresponding author upon request.

#### Conflicts of Interest

The authors declare that there are no conflicts of interest regarding the publication of this paper.

#### Acknowledgments

This work was supported by Prof. Zengcai Wang. Zengfu Yang would like to show sincere gratitude to Prof. Zengcai Wang, who has given so much useful advice on writing and has tried his best to improve the paper.

#### References

- [1] S. Miao and X. Liu, "Free radical characteristics and classification of coals and rocks using electron spin resonance spectroscopy," *Journal of Applied Spectroscopy*, vol. 86, no. 2, pp. 345–352, 2019.
- [2] Li Li, J. Liu, and W. Wei, "Signal processing method on ultrasonic echo from coal-rock interface based on EWTP," *Journal of China Coal Society*, vol. 44, no. S1, pp. 370–377, 2019.
- [3] G. Mowrey, "Horizon control holds key to automation," *Coal*, vol. 97, no. 1, pp. 44–49, 1992.
- [4] D. Law, "Auto-steerage—an aid to production, pt. 1," *Mining Engineer*, vol. 148, pp. 326–334, 1989.
- [5] J. Qin, J. Zheng, X. Zhu, and D. Shi, "Establishment of a theoretical model of sensor for identification of coal rock interface by natural ray and underground trials," *Journal of China Coal Society*, vol. 21, no. 5, pp. 513–516, 1996.
- [6] Z. C. Wang, R. L. Wang, and J. H. Xu, "Research on coal seam thickness detection by natural Gamma ray in shearer horizon control," *Journal of China Coal Society*, vol. 27, no. 4, pp. 425–429, 2002.
- [7] A. D. Strange, "Robust Thin Layer Coal Thickness Estimation Using Ground Penetrating Radar", Queensland University of Technology, Brisbane, Queensland, 2007.
- [8] S. Maksimovic and G. Mowrey, "Basic geological and analytical properties of selected coal seams for coal interface detection. Information circular," in *Book Basic Geological and Analytical Properties of Selected Coal Seams for Coal Interface Detection. Information Circular*, Bureau of Mines, Pittsburgh Research Center, Pittsburgh, PA, USA, 1993.

- [9] F. Ren, Z. Liu, and Z. Yang, "Harmonic response analysis on cutting part of shearer physical simulation system paper title," in *Book Harmonic Response Analysis on Cutting Part of Shearer Physical Simulation System Paper Title*, pp. 2509–2513, IEEE, Piscataway, NY, USA, 2010.
- [10] Y. X. Gao and X. L. Lu, "The optimization of shearer's memory cutting system based on mechanical characteristics of cutting tooth," *Journal of Liaoning Technical University(Natural Science)*, vol. 35, no. 6, p. 3, 2016.
- [11] G. Zhang, Z. Wang, L. Zhao, Y. Qi, and J. Wang, "Coal-rock recognition in top coal caving using bimodal deep learning and hilbert-huang transform," *Shock and Vibration*, vol. 2017, Article ID 3809525, 13 pages, 2017.
- [12] L. Si, Z. Wang, X. Liu, C. Tan, and L. Zhang, "Cutting state diagnosis for shearer through the vibration of rocker transmission part with an improved probabilistic neural network," *Sensors*, vol. 16, no. 4, p. 479, 2016.
- [13] J. Sun and B. Su, "Coal-rock interface detection on the basis of image texture features," *International Journal of Mining Science and Technology*, vol. 23, no. 5, pp. 681–687, 2013.
- [14] S. Jiping, "Study on identified method of coal and rock interface based on image identification," *Coal Science and Technology*, vol. 39, no. 2, pp. 77–79, 2011.
- [15] Y.-x. Wu and Y.-m. Tian, "Method of coal-rock image feature extraction and recognition based on dictionary learning," *Journal of China Coal Society*, vol. 41, no. 12, 2016.
- [16] N. Zhang, C. Liu, X. Chen et al., "Measurement analysis on the fluctuation characteristics of low level natural radiation from gangue," *Journal of China Coal Society*, vol. 40, no. 5, pp. 988–993, 2015.
- [17] S. L. Bessinger and M. G. Nelson, "Remnant roof coal thickness measurement with passive gamma ray instruments in coal mines," *IEEE Transactions on Industry Applications*, vol. 29, no. 3, pp. 562–565, 1993.
- [18] Y. Yu, Y. Lun, W. S. Liu, and G. C. Feng, "Quadratic function analysis of greatest subsidence angle during mining pitching or steerly pitching coal seam," *Journal of Liaoning Technical University*, vol. 24, no. 5, 2005.
- [19] G. Ji, D. Li, and X. Wu, "Study of rules of natural  $\gamma$ RAYS passing through coal seam," *Journal of China Coal Society*, vol. 19, no. 1, 1994.
- [20] O. P. Hackney, "An introduction to probability theory and mathematical statistics," *American Statistician*, vol. 21, no. 3, pp. 331–332, 2002.
- [21] J. M. Zhang, L. I. Wen-Bin, X. Fan, and F. Y. Kang, "Automatic Control System of Height Setting of Shearer Based on Single-Chip Microcomputer", Inoustry & Mine Automation, Beijing, China, 2004.
- [22] W. Boyes, "Instrumentation Reference Book", Butterworth-Heinemann, Oxford, UK, 2009.
- [23] M. Borsaru, M. Biggs, W. Nichols, and F. Bos, "The application of prompt-gamma neutron activation analysis to borehole logging for coal," *Applied Radiation and Isotopes*, vol. 54, no. 2, pp. 335–343, 2001.